Acta Crystallographica Section F
Structural Biology and Crystallization Communications
ISSN 1744-3091

Crystallization and preliminary X-ray analysis of the human androgen receptor ligand-binding domain with a coactivator-like peptide and selective androgen receptor modulators

Maxime Thauvin,[a,b] Catherine Robin-Jagerschmidt,[b]‡ François Nique,[b]‡ Patrick Mollat,[b]‡ Damien Fleury[b]‡ and Thierry Prangé[a]*

[a]UMR 8015 CNRS, Université Paris Descartes, 4 Avenue de l'Observatoire, 75006 Paris, France, and [b]Proskelia, Parc Biocitech, 102 Avenue G. Roussel, 93230 Romainville, France

‡ Present address: Galapagos SASU, Parc Biocitech, 102 Avenue G. Roussel, 93230 Romainville, France.

Correspondence e-mail: thierry.prange@univ-paris5.fr

Received 26 August 2008
Accepted 7 November 2008

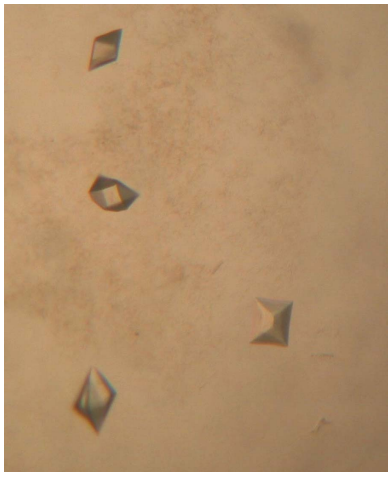

The ligand-binding domain of the human androgen receptor has been cloned, overproduced and crystallized in the presence of a coactivator-like 11-mer peptide and two different nonsteroidal ligands. The crystals of the two ternary complexes were isomorphous and belonged to space group $P2_12_12_1$, with one molecule in the asymmetric unit. They diffracted to 1.7 and 1.95 Å resolution, respectively. Structure determination of these two complexes will help in understanding the mode of binding of selective nonsteroidal androgens *versus* endogenous steroidal ligands and possibly the origin of their tissue selectivity.

1. Introduction

The androgen receptor (AR) is a ligand-inducible steroid hormone receptor that is widely distributed throughout the body and is involved in diverse transcriptional regulation pathways. The function of AR is regulated by the binding of androgens, which initiates sequential conformational changes of the receptor that affect receptor–protein interactions and receptor–DNA interactions.

Androgens act on most body tissues and have a variety of biological effects. They stimulate prenatal differentiation of male reproductive tissues and their development during puberty. In adults, androgens, which are required for the maintenance of these tissues, play a key role in stimulating sexual function in men (Collins *et al.*, 2003; Gottlieb *et al.*, 2005; Heinlein & Chang, 2002; Pelletier, 2000).

With increasing life expectancy, it can be anticipated that osteoporosis in men, and its clinical end point of fracture, will rapidly become an issue for public healthcare. There is general agreement that testosterone-replacement therapy (TRT) has a protective effect on bone mass and improves muscle strength. Indeed, TRT has been shown to normalize bone-mineral density and biochemical parameters of bone turnover in hypogonadal (Snyder *et al.*, 2000; Wang *et al.*, 2004) or aged men (Snyder *et al.*, 1999; Szulc *et al.*, 2000). In addition, testosterone has also been shown to be beneficial in HIV-induced cachexia (Bhasin *et al.*, 2000). The main issues surrounding TRT relate to an increase in the risk of clinically progressive prostate carcinoma as well as the precipitation or exacerbation of benign prostatic hyperplasia. They also include an increase in the haematocrit owing to persistent erythropoietic stimulation and a tendency toward thrombosis. In addition, the effects of androgens on lipid metabolism need to be further clarified. The potential adverse effects of androgens compromise their prolonged utilization (reviewed in Gooren, 2003).

Androgens can be classified as steroidal or nonsteroidal based on their structure. Endogenous androgens and modified steroidal ligands have some shortcomings that limit their general use, mainly their potential for generating side effects and their mode of administration; owing to their high hepatic first-pass metabolism, endogenous steroidal androgens can only be administered either by intramuscular injections or transdermal patches. Potential uses of androgens include male hormone-replacement therapy, male contraception and treatment of bone disorders, wasting diseases and female androgen deficiency, amongst many others. In contrast to agonists, nonsteroidal androgen antagonists have been marketed for many years (Labrie, 1993; Hamann *et al.*, 1998) and are currently used in the treatment of

prostate cancer (Suzuki *et al.*, 2008). Possible other indications include benign prostatic hyperplasia and androgen-dependent disorders such as acne, androgenic alopecia and hirsutism. Theoretically, androgen therapy could be almost as widely used as female sex-hormone therapies, but this would require more selective and effective therapeutic agents.

In this context, the development of selective androgen receptor modulators (SARMs) with intrinsic partial agonist activity offers an opportunity to characterize new therapeutic agents with tissue-selective activity profiles, *i.e.* molecules that will prevent bone loss, stimulate new bone formation and muscle growth and, conversely, have a reduced stimulatory effect on the prostate (Rosen & Negro-Vilar, 2002; van Oeveren *et al.*, 2006). To gain further insight into the structure–activity relationships of androgens and to determine whether we can explain the behaviour of two ligands we have developed on a structural basis, a structural study of complexes formed with the human AR ligand-binding domain (hAR LBD) was undertaken.

2. Material and methods

2.1. Cloning and expression

The cDNA encoding the ligand-binding domain (LBD; amino acids 663–919) of the human androgen receptor was cloned C-terminally to a thioredoxin-6His cassette in a modified pET32a vector. A thrombin cleavage site was inserted between the thioredoxin-6His and the LBD, which allowed both purification with and release of the thioredoxin-6His moiety. *Escherichia coli* BL21 (DE3) bacteria were transformed and plated on solid Luria–Bertani medium supplemented with 100 µg ml^{-1} ampicillin as a selection agent. Colonies were grown at 310 K. The best expressing colony was selected and used to inoculate 5 l fermentors.

Typically, 3 l bacterial culture was grown at 310 K in Luria–Bertani medium containing 50 µg ml^{-1} ampicillin and enriched with 5%(*v*/*v*) glycerol. When the $OD_{600\,nm}$ reached 2.3, the incubation temperature was linearly decreased to 289 K and 10 µ*M* of ligand (final concentration) was added. The culture was grown at 289 K until the $OD_{600\,nm}$ reached 2.5. At this point, induction was performed by the addition of isopropyl *β*-D-1-thiogalactopyranoside to a final concentration of 0.5 m*M* and the culture was left to grow overnight. The final $OD_{600\,nm}$ reached 13–17. Cells were harvested and kept at 193 K until use.

2.2. Purification

The purification protocols used to obtain both the LBD–ligand-1 and LBD–ligand-2 complexes (Fig. 1) were similar. All operations were performed at 277 K unless specified. The syntheses of the ligands will be reported elsewhere.

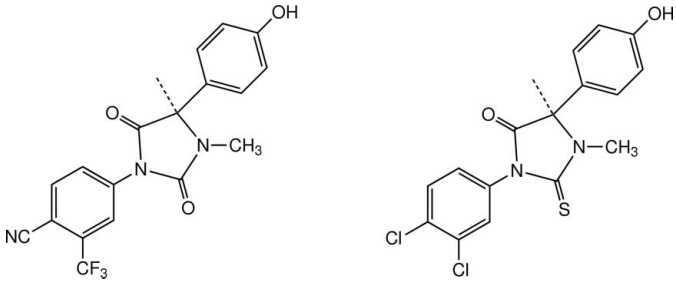

Figure 1
Planar formulae of ligand-1 (left) and ligand-2 (right).

A frozen pellet of 30 g was resuspended in four volumes of lysis buffer (50 m*M* Tris pH 8, 100 m*M* NaCl) supplemented with EDTA-free protease-inhibitor cocktail tablets (one tablet per 50 ml). After homogenization at 277 K, the sample was sonicated in an ice-water bath for 45 min.

After sonication, the volume was adjusted to 180 ml with lysis buffer. NaCl powder and 2 *M* imidazole solution were added to achieve final concentrations of 400 m*M* and 20 m*M*, respectively. This sample was submitted to ultracentrifugation at 140 000*g* at 277 K for 1 h. The supernatant was loaded at 2.5 ml min^{-1} onto a 5 ml HisTrap column (GE Healthcare) equilibrated in a buffer containing 50 m*M* Tris pH 8.0, 400 m*M* NaCl, 20 m*M* imidazole and 10 µ*M* ligand. To remove contaminants, the column was washed first with a buffer containing 50 m*M* Tris pH 8, 400 m*M* NaCl and 40 m*M* imidazole and then with the same buffer containing 80 m*M* imidazole. The protein was eluted from the column with a linear gradient of imidazole (to 500 m*M*). To avoid precipitation owing to too high a concentration of protein during elution, 1 ml fractions were collected in a 96-well plate containing 1 ml buffer solution (50 m*M* Tris pH 7.5, 50 m*M* NaCl, 10% glycerol and 1 m*M* EDTA) per well. The presence of the protein was checked on a pre-casted SDS NuPAGE gel (Invitrogen) stained with Coomassie blue. Fractions containing the thioredoxin-6His-hAR LBD were pooled.

The cleavage was performed by thrombin, which was added to 25 U per milligram of protein and incubated overnight at 277 K without agitation. Imidazole from the previous step was removed by dialysis against a buffer containing 50 m*M* Tris pH 7.5, 50 m*M* NaCl, 10%(*v*/*v*) glycerol, 0.5 m*M* DTT and 5 µ*M* ligand. The mixture was loaded at 2.5 ml min^{-1} onto a 5 ml HisTrap column equilibrated in the same buffer plus 5 µ*M* ligand. Surprisingly, hAR LBD reproducibly binds to the column even without the His tag and was eluted with a buffer containing 50 m*M* Tris pH 7.5, 50 m*M* NaCl, 10%(*v*/*v*) glycerol, 0.5 m*M* DTT, 40 m*M* imidazole and 5 µ*M* ligand (Fig. 2).

Finally, the sample was directly loaded onto a 5 ml HiTrap SP (GE Healthcare) equilibrated in the previous buffer but without imidazole and eluted by an increasing NaCl concentration to 0.25 *M*. The purity of the protein was again checked on an SDS NuPAGE gel stained

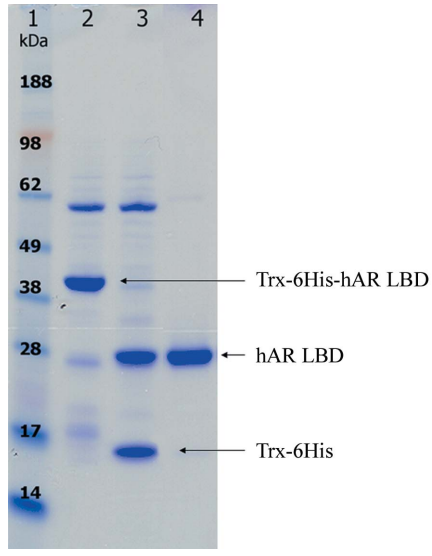

Figure 2
SDS–PAGE gel of thrombin cleavage of the fusion product and purification on HisTrap. Lane 1, SeeBlue+2 molecular-mass markers (Invitrogen); lane 2, Trx-6His-hAR LBD; lane 3, after cleavage by thrombin; lane 4, purified hAR LBD after second HisTrap, theoretical molecular mass 29 977 Da.

with Coomassie blue. Fractions containing the hAR LBD–ligand complex were pooled to yield final batches of protein of about 15 mg at a concentration of 3.5 mg ml^{-1}.

2.3. Crystallization

Three hits were found using Hampton Research Crystal Screen 2 with a crystallization robot. All three included lithium sulfate as a cocrystallizing agent. One of these conditions gave small single crystals that were further used for seeding in optimized conditions. Optimization was achieved in Linbro boxes. The best crystals (Fig. 3) were obtained in hanging drops with the following conditions. The protein solution consisted of 80 µl hAR LBD (3.5 mg ml^{-1}), 1.5 µl ligand (10 m*M*), 3 µl of the co-activator-like F*xx*LF motif-containing undecapeptide from hAR (He *et al.*, 2000), *i.e.* GAFQNLFQSVR (20 m*M*) and 1 µl lithium sulfate (0.2 *M*). All solutions were in HEPES buffer pH 7.5.

Reservoirs were set up in five rows with solutions of 1 ml 0.1 *M* HEPES Na buffer pH 7.5 and a gradient of 12–20% PEG 4000 (in five steps).

The hanging drop was set up as a 50:50 mixture of 1 µl protein solution and 1 µl reservoir solution. Small bipyramidal crystals were obtained in 1 or 2 d with maximum dimensions of 100–150 µm. All attempts to use additives or to vary the temperature or the pH did not yield larger crystals. However, we found that the co-activator-like undecapeptide and lithium sulfate as well as the synthetic ligand were all compulsory for obtaining crystals.

2.4. X-ray diffraction

Data sets were recorded at the ESRF (Grenoble, France). Several cryoprotectants were tested, including ethylene glycol, methyl pentanediol and PEG 400 at different concentrations. The best combination found was a 10% gycerol solution of the reservoir in each case. Crystals were soaked in this solution for a few minutes and then rapidly transferred into the cold gas stream of an Oxford Cryosystem (600 Series Cryostream Cooler) at 100 K. The crystals usually diffracted moderately, with a maximum resolution of around 2.8–3.5 Å and poor spot shapes, except for a very small number of them that showed diffraction spots at a resolution better than 2 Å. We were able to collect data from two such crystals. Data-collection statistics are reported in Table 1.

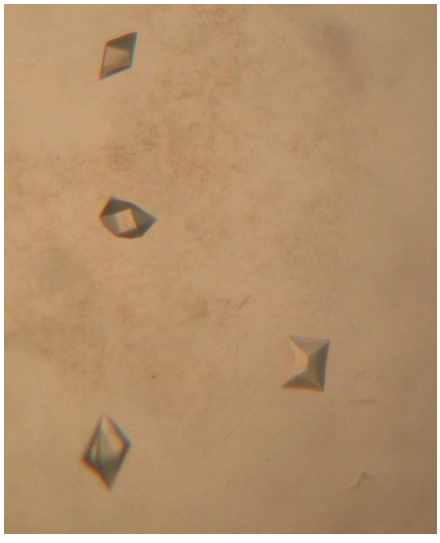

Figure 3
Bipyramidal crystals of the ternary complex hAR LBD–undecapeptide–ligand-1.

Table 1
Data-collection statistics.

Values in parentheses are for the highest resolution shell.

Data set	hAR LBD–coactivator-like peptide–ligand-1	hAR LBD–coactivator-like peptide–ligand-2
Beamline	ID23-1	ID14 EH1
Wavelength (Å)	0.934	0.922
Detector	ADSC 315R	ADSC Q210
Crystal-to-detector distance (mm)	170	180
Exposure time per rotation (s)	2	1
Frame rotation (°)/Total rotation (°)	1/360	1/250
Space group	$P2_12_12_1$	$P2_12_12_1$
Unit-cell parameters (Å)	a = 54.63, b = 67.33, c = 69.81	a = 54.45, b = 66.80, c = 69.85
Matthews coefficient (Å^3 Da^{-1})	2.14	2.10
Solvent content (%)	42.5	41.1
Resolution limits (Å)	34.9–1.70 (1.80–1.70)	36.1–1.95 (2.10–1.95)
Overall $\langle I/\sigma(I)\rangle$	29.6 (7.5)	35.5 (5.4)
No. of measured reflections	458718	225123
Overall redundancy	7.9	3.7
$R_{\rm merge}$† (%)	4.34 (18.50)	5.12 (19.30)
Completeness (%)	98.3 (97.6)	99.5 (97.8)
No. of independent reflections	28377 (4413)	20128 (4330)
No. of independent observed reflections	28211 (4340)	18995 (3752)

† Defined as $\sum_{hkl}\sum_i |I_i(hkl) - \langle I(hkl)\rangle|/\sum_{hkl}\sum_i I_i(hkl)$, where $I_i(hkl)$ is the ith observation of reflection hkl and $\langle I(hkl)\rangle$ is the weighted mean of all observations (after rejection of outliers).

3. Results

We produced and purified to homogeneity hAR LBD–ligand complexes in quantities and with qualities that were suitable for crystallogenesis. For the production, the critical point was the addition of ligand to the culture medium before induction, as described previously (Sack *et al.*, 2001). In the absence of any ligand, almost all the protein was found in inclusion bodies (data not shown). To ensure the stability of the protein, ligand was added throughout the purification procedure (except for lysis). Cleavage of the thioredoxin-fusion product by thrombin was efficient and the purification process allowed us to obtain large amounts (>15 mg) of pure protein–ligand complexes for use in screening for crystallization conditions.

We noticed that the two LBD–ligand complexes showed notable differences in diffraction limits, lifetime and stability in the X-ray beam. The corresponding data sets were processed using *MOSFLM* (Leslie, 1992) and scaled using the *CCP*4 package of programs (Collaborative Computational Project 4, Number 4, 1994). Both structures were solved by molecular replacement using PDB entry 2ama (Pereira de Jésus-Tran *et al.*, 2006) without ligand as a starting model (Navaza, 1994). In both cases, a unique solution was found. The structures are being refined.

The staff scientists of the ESRF beamlines are acknowledged for their help during data collection. We thank Jean-Michel Lemoullec from Galapagos for excellent assistance in providing us with the expression vector.

References

Bhasin, S., Storer, T. W., Javanbakht, M., Berman, N., Yarasheski, K. E., Phillips, J., Dike, M., Sinha-Hikim, I., Shen, R., Hays, R. D. & Beall, G. (2000). *JAMA*, **283**, 763–770.
Collaborative Computational Project, Number 4 (1994). *Acta Cryst.* D**50**, 760–763.

Collins, L. L., Lee, H. J., Chen, Y. T., Chang, M., Hsu, H. Y., Yeh, S. & Chang, C. (2003). *Cytogenet. Genome Res.* **103**, 299–301.
Gooren, L. (2003). *J. Steroid. Biochem. Mol. Biol.* **85**, 349–355.
Gottlieb, B., Lombroso, R., Beitel, L. K. & Trifiro, M. A. (2005). *Reprod. Biomed. Online*, **10**, 42–48.
Hamann, L. G., Winn, D. T., Pooley, C. L., Tegley, C. M., West, S. J., Farmer, L. J., Zhi, L., Edwards, J. P., Marschke, K. B., Mais, D. E., Goldman, M. E. & Jones, T. K. (1998). *Bioorg. Med. Chem. Lett.* **8**, 2731–2736.
He, B., Kemppainen, J. A. & Wilson, E. M. (2000). *J. Biol. Chem.* **275**, 22986–22994.
Heinlein, C. A. & Chang, C. (2002). *Endocr. Rev.* **23**, 175–200.
Labrie, F. (1993). *Cancer*, **72**, 3816–3827.
Leslie, A. G. W. (1992). *Jnt CCP4/ESF–EACBM Newsl. Protein Crystallogr.* **26**.
Navaza, J. (1994). *Acta Cryst.* A**50**, 157–163.
Oeveren, A. van, Motamedi, M., Mani, N. S., Marschke, K. B., López, F. J., Schrader, W. T., Negro-Vilar, A. & Zhi, L. (2006). *J. Med. Chem.* **49**, 6143–6146.
Pelletier, G. (2000). *Histol. Histopathol.* **5**, 1261–1270.
Pereira de Jésus-Tran, K., Cote, P. L., Cantin, L., Blanchet, J., Labrie, F. & Breton, R. (2006). *Protein Sci.* **15**, 987–999.
Rosen, J. & Negro-Vilar, A. (2002). *J. Musculoskelet. Neuronal Interact.* **3**, 222–224.
Sack, J. S., Kish, K. F., Wang, C., Attar, R. M., Kiefer, S. E., An, Y., Wu, G. Y., Scheffler, J. E., Salvati, M. E., Krystek, S. R. Jr, Weinmann, R. & Einspahr, H. M. (2001). *Proc. Natl Acad. Sci. USA*, **98**, 4904–4909.
Snyder, P. J., Peachey, H., Berlin, J. A., Hannoush, P., Haddad, G., Dlewati, A., Santanna, J., Loh, L., Lenrow, D. A., Holmes, J. H., Kapoor, S. C., Atkinson, L. E. & Strom, B. L. (1999). *J. Clin. Endocrinol. Metab.* **84**, 1966–1972.
Snyder, P. J., Peachey, H., Berlin, J. A., Hannoush, P., Haddad, G., Dlewati, A., Santanna, J., Loh, L., Lenrow, D. A., Holmes, J. H., Kapoor, S. C., Atkinson, L. E. & Strom, B. L. (2000). *J. Clin. Endocrinol. Metab.* **85**, 2670–2677.
Suzuki, H., Kamiya, N., Imamoto, T., Kawamura, K., Yano, M., Takano, M., Utsumi, T., Naya, Y. & Ichikawa, T. (2008). *Int. J. Clin. Oncol.* **13**, 401–410.
Szulc, P., Marchand, F., Duboeuf, F. & Delmas, P. D. (2000). *Bone*, **26**, 123–129.
Wang, C., Cunningham, G., Dobs, A., Iranmanesh, A., Matsumoto, A. M., Snyder, P. J., Weber, T., Berman, N., Hull, L. & Swerdloff, R. S. (2004). *J. Clin. Endocrinol. Metab.* **89**, 2085–2098.